


Article

Modulation Recognition System of Electromagnetic Interference Signal Based on SDR

Wei Dai *  and Changpeng Ji

School of Electronics and Information Engineering, Liaoning Technical University, Huludao 125105, China; jichangpeng@163.com

* Correspondence: daiwei0084@126.com

Abstract: Considering the electromagnetic interference signal in non-cooperative communication, an automatic modulation identification and detection system of electromagnetic interference signal based on software defined radio is proposed. Based on GNU Radio 3.10.7.0 and HackRF One B210mini,, the system estimates the frequency and symbol rate of the interference signal and completes clock synchronization and matching filtering under the condition of unknown a priori information. By extracting high-order cumulants as characteristic parameters, combined with the decision tree classifier, the classification and recognition of six modulation types of interference signals and signal phase correction are realized. This method can distinguish the recognition results in combination with the signal constellation, and complete the real-time reception and recognition of interference signals.

Keywords: software defined radio; parameter estimation; modulation identification; higher order cumulant; decision tree

1. Introduction

In the field of non-cooperative communication, modulation recognition means that the receiver automatically recognizes the modulation type of the signal without prior knowledge and noise interference. Combining software defined radio, which, as a multifunctional radio communication platform with modulation recognition technology, can effectively realize the automatic reception and recognition of communication signals, and improve the universality and practicability of modulation recognition [1,2].

At present, the methods of modulation recognition mainly include maximum likelihood based on hypothesis testing and pattern recognition based on feature extraction. Kim [3], Lay [4], Panagiotors [5], Dobre [6], Wu B [7], and other scholars have used the maximum likelihood method to study the modulation recognition technology. This method judges the modulation category of the signal by analyzing the statistical characteristics of the modulation signal. However, the computational complexity is high and the scope of application is narrow. Moreover, in the process of recognition, this method needs to master the prior information, such as signal frequency, baud rate, and signal-to-noise ratio, which is difficult to obtain accurately in the field of non-cooperative communication.

The pattern recognition method based on feature extraction is to extract the characteristic parameters different from other modulation signals from the received signals, and then use the classifier to classify them to determine the modulation type of the signals. Common features include: wavelet domain features [8,9], cyclic spectrum [10–12], and higher order cumulant [13–18].

Wang L [13] proposed a method combining high-order cumulant with support vector machine to successfully identify 2ASK, 4ASK, QPSK, 2FSK, and 4FSK signals. Zhang Li [15] extracted the combination of second-order and eighth-order cumulants as characteristic parameters, and combined with support vector machine to realize the modulation recognition of mask, MPSK, MFSK, and MQAM signals. When the signal-to-noise ratio is 10 dB, the



Citation: Dai, W.; Ji, C. Modulation Recognition System of Electromagnetic Interference Signal Based on SDR. *Telecom* **2024**, *5*, 928–940. <https://doi.org/10.3390/telecom5030046>

Academic Editor: Minseok Kim

Received: 9 August 2024

Revised: 6 September 2024

Accepted: 6 September 2024

Published: 11 September 2024



Copyright: © 2024 by the authors. Licensee MDPI, Basel, Switzerland. This article is an open access article distributed under the terms and conditions of the Creative Commons Attribution (CC BY) license (<https://creativecommons.org/licenses/by/4.0/>).

accuracy can reach 100%. Weng J X [16] took the combination of high-order cumulants as characteristic parameters and combined this with the random forest classification method to realize the inter class and intra class recognition of MPSK, MQAM, and MAPSK signals. Ali a K [17] used the method of higher-order cumulant and logarithm to classify the modulation of MQAM. Yuan L [18] combined high-order cumulant with a deep-learning method to realize four kinds of classification first, and then processed by high-order cumulant for in class recognition. Liu Zhao Yang [19] used high-order cumulants to identify BPSK, 8PSK, and 16QAM signals under low SNR in non-cooperative communication.

The above studies mostly identify the signals in the standard database, but do not consider that the signals in the actual environment may be affected by the acquisition environment, acquisition mode, etc. Ref. [20] first collects signals in space through SDR equipment, and then uses an artificial intelligence classifier to train and recognize the collected signals. The amount of computation of the artificial intelligence classifier is large, and the real-time performance is not as good as the decision tree classifier.

Therefore, according to the demand for real-time performance in engineering applications, combining software radio with modulation identification technology, an automatic modulation identification, and a detection system of electromagnetic interference signal based on SDR is proposed to realize the automatic detection and identification of six modulation types of electromagnetic interference signal modulation modes in space: BPSK, QPSK, 8PSK, 8QAM, 16QAM, and 64QAM.

2. Modulation Recognition System

Modulation recognition refers to the classification and judgment of the modulation type of the signal according to its relevant characteristics under the condition of unknown target signal information, including signal pre-processing, feature extraction, classification, and recognition, as shown in Figure 1.

The modulation signal pre-processing is to estimate the frequency and symbol rate of the signal, complete clock synchronization, and perform matching filtering, so that the received signal can remove some interference, and provide easier signal data for later feature extraction and classification and recognition.

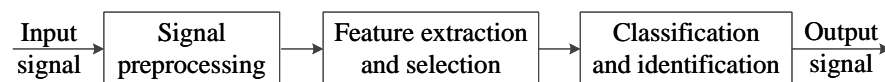


Figure 1. The structure of the software radio modulation recognition system.

In the communication system, the signal $r(t)$ received by the receiver can be expressed.

$$\begin{aligned} r(t) &= s(t) + n(t) \\ &= \sqrt{E} \sum_n s[nT]g(t - nT)e^{j(\omega_c t + \theta_c)} + n(t) \end{aligned} \quad (1)$$

where $s[nT]$ is the transmitted symbol sequence, E is the symbol energy, $g(t)$ is the symbol waveform, ω_c is the carrier frequency, θ_c is the carrier phase, and $n(t)$ is Gaussian white noise.

Before identifying the received interference signal, first pre-process the interference signal, estimate the signal frequency and symbol rate, and complete clock synchronization and matching filtering.

The position of the discrete spectral line of the modulation signal contains the frequency and symbol rate information of the signal, so the frequency and symbol rate of the signal can be estimated according to the spectral line position of each modulation signal. The modulation signal $s(t)$ is constructed as a cyclostationary random process, and its time-varying autocorrelation function is expressed.

$$R_s(t; \tau) = E[s(t)s^*(t - \tau)] \quad (2)$$

If $R_s(t; \tau)$ has the statistical characteristic with the time period T_0 , then $s(t)$ is called a second-order cyclostationary process and Equation (3) can be obtained.

$$\begin{cases} R_s(t; \tau) = \sum_m R_s^\alpha(\tau) \exp(j2\pi\alpha t) \\ R_s^\alpha(\tau) = \frac{1}{T_0} \int_{-\frac{T_0}{2}}^{\frac{T_0}{2}} R_s(t; \tau) \exp(-j2\pi\alpha t) dt \end{cases} \quad (3)$$

where, $\alpha = m/T_0$, ($m = 0, 1, 2, 3 \dots$) is the cycle frequency. Since $R_s(t; \tau)$ has periodic time variability, so the signal will appear discrete spectral lines in the frequency domain, which is called the spectral characteristics of the signal. When $\tau = 0$, the statistical expected value $R_s(t; 0)$ of the quadratic power of the signal.

$$u(t) = R_s(t; 0) = E[s^2(t)] \quad (4)$$

The quadratic spectrum of the signal is obtained by Fourier transform: $U(f) = F\{E[s^2(t)]\}$.

Similarly, the fourth power spectrum $V(f) = F\{E[s^4(t)]\}$ and eighth power spectrum of the signal $W(f) = F\{E[s^8(t)]\}$ can be obtained.

Different modulation signals have different spectral line characteristics in each order of power spectrum. Taking QPSK as an example, when the modulation order $M = 4$, the information sequence of QPSK signal is $\theta = \{\pi/4, 3\pi/4, 5\pi/4, 7\pi/4\}$, so the statistical expectation of the quadratic form of QPSK signal is equal to 0.

$$\begin{aligned} E[s^2(t)] &= E\left[\sum_n \sum_m (a_n + jb_n)(a_m + jb_m)g(t - nT)g(t - mT)\right] \\ &= \sum_n E[a_n^2 - b_n^2]g(t - nT) \end{aligned} \quad (5)$$

According to Equation (5), $E[s^2(t)]$ does not have periodic characteristics, so there is no discrete spectral line in the quadratic spectrum of QPSK signal. The quartic statistical expected value of QPSK signal can be expressed.

$$\begin{aligned} E[s^4(t)] &= E\left[\sum_n \left[a_n^4 + b_n^4 - 2a_n^2 b_n^2\right]g^4(t - nT)\right] \\ &= \left(-E_s^2\right)g^4(t - nT) \end{aligned} \quad (6)$$

where E_s is the symbolic average energy. The quartic spectrum of QPSK signal can be obtained by Fourier transform of Equation (6).

$$\begin{aligned} V(f) &= -\frac{E_s^2}{T^4} \sum_n A(f) \delta\left(f - \frac{n}{T}\right) \\ A(f) &= G(f) * G(f) * G(f) * G(f) \end{aligned} \quad (7)$$

where, $G(f)$ is the Fourier transform of $g(t)$ and $*$ represents linear convolution. According to the property of rising cosine pulse, the spectral band limited interval of quadratic spectrum is $[-2(1 + \alpha)/T, 2(1 + \alpha)/T]$. Under the conditions of roll off coefficient $\alpha < 0.5$, $n \in \{0, \pm 1, \pm 2\}$, therefore, the fourth power spectrum $V(f)$ of QPSK has non-zero values only at the frequencies $f \in \{0, \pm 1/T, \pm 2/T\}$, that is, there are discrete spectral lines. Due to the attenuation of $A(f)$, the discrete spectral line intensity at frequency $f = \pm 2/T$ is much less than that at frequency $f = \{0, \pm 1/T\}$.

For quadrature amplitude-modulated QAM signals with symmetrical origin and equal probability distribution, the statistical expectations in the form of quadratic and quartic spectra.

$$E[s^2(t)] = E[s^8(t)] \quad (8)$$

$$E[s^4(t)] = (-E_s^2) \sum_n g^4(t - nT) \quad (9)$$

It can be seen that different kinds of modulation signals have discrete spectral lines in different high-power spectra. For example, the 16QAM signal has obvious discrete spectral lines in the fourth power spectrum, while the 8PSK signal only has obvious discrete spectral lines in the eighth power spectrum. Therefore, to estimate the frequency and symbol rate of each modulated signal, it is necessary to calculate the quadratic spectrum, the quartic spectrum, and the eighth spectrum of the signal, calculate the peak-to-average ratio of the spectral line of the signal in the three spectra, respectively, and find the spectrum where the maximum peak-to-average ratio is located. The discrete spectral line position corresponding to the maximum peak-to-average ratio in the spectrum is the estimated value of the signal frequency. The distance between the position of the spectral line corresponding to the maximum value and the second maximum value of the peak-to-average ratio is the estimated value of the signal symbol rate.

3. High Order Cumulant Modulation Recognition Model

Modulation signal feature extraction is designed to extract the feature information that can reflect the signal modulation type from the pre-processed signal sequence and use it for classification and recognition. Because the higher-order cumulant of the Gaussian random variable is equal to zero, the higher-order cumulant is used as the characteristic parameter in modulation recognition to remove the influence of Gaussian white noise and improve the anti-noise performance. At the same time, combined with the decision tree classifier, the classification and recognition of modulation signals other than 16QAM and 64QAM signals are realized by step-by-step processing.

For the random variable X , whose probability density function is $f(X)$, its first characteristic function $\Phi(\omega)$ is expressed.

$$\begin{aligned} \Phi(\omega) &= E\{\exp(j\omega X)\} \\ &= \int_{-\infty}^{\infty} f(X) \exp(j\omega X) dX \end{aligned} \quad (10)$$

The k -order moment m_k of random variable X is expressed.

$$m_k = E\{X^k\} = \int_{-\infty}^{\infty} X^k f(X) dX \quad (11)$$

By finding the k -order derivative of Equation (10), Equation (12) can be obtained.

$$\Phi^k(\omega) = \frac{d^k \Phi(\omega)}{d\omega^k} = j^k E\{X^k \exp(j\omega X)\} \quad (12)$$

According to Equations (11) and (12), when $\omega = 0$, the k -order moment formula of random variable X can be obtained.

$$m_k = E\{X^k\} = (-j)^k \left. \frac{d^k \Phi(\omega)}{d\omega^k} \right|_{\omega=0} = (-j)^k \Phi^{(k)}(0) \quad (13)$$

By performing natural logarithm operation on the first characteristic function $\Phi(\omega)$, the second characteristic function can be obtained.

$$\Psi(\omega) = \ln \Phi(\omega) \quad (14)$$

Similarly, the calculation formula of the k -order moment of the second characteristic function can be deduced as follows.

$$c_k = (-j)^k \left. \frac{d^k \ln \Phi(\omega)}{d\omega^k} \right|_{\omega=0} = (-j)^k \Psi^{(k)}(0) \tag{15}$$

where c_k is the k-order cumulant of random variable X.

For a stationary continuous random process with multiple random variables, the k-order moment and the k-order cumulant of the random signal $X(t)$ can be obtained.

$$m_{kx}(\tau, \dots, \tau_{k-1}) = \text{mom}[X(t), \dots, X(t + \tau_{k-1})] \tag{16}$$

$$c_{kx}(\tau, \dots, \tau_{k-1}) = \text{cum}[X(t), \dots, X(t + \tau_{k-1})] \tag{17}$$

where mom represents the joint moment and cum represents the joint cumulant.

If $X(t)$ is a complex stationary random process, the expression of its p-order q-order mixing moment can be defined.

$$M_{pq} = E \left[X(t)^{p-q} (X^*(t))^q \right] \tag{18}$$

where * represents conjugation. The $X(t)$ higher-order cumulant is defined.

$$c_{pq} = \text{cum} \left[X(t), \dots, X(t), X^*(t), \dots, X^*(t) \right] \tag{19}$$

where the number of $X(t)$ is $p-q$ and the number of $X^*(t)$ is q . At the same time, there is a mutual conversion relationship between higher-order moment and higher-order cumulant function.

$$\text{cum}(X_1, \dots, X_k) = \sum_n (-1)^{q-1} (q-1)! \prod_{p=1}^q E \left(\prod_{l \in U_p} X_l \right) \tag{20}$$

Equation (20) is called moment–cumulant conversion formula, i.e., M–C formula, where $X_l, l = 1, 2, \dots, k$ are k stationary random variables and $\Sigma(\bullet)$ represents the sum of all unconnected ordered partitioned sets $X = (X_1, X_2, \dots, X_k)$. Up is the subscript set of the elements in the p -th subset of the q -th subset.

For zero mean complex random process $X(t)$, the relationship between the second to sixth order cumulants and their higher-order moments can be obtained from the M–C formula: $C_{20} = M_{20}$; $C_{21} = M_{21}$, $C_{40} = M_{40} - 3M_{20}^2$, $C_{41} = M_{41} - 3M_{21}M_{30}$, $C_{42} = M_{42} - |M_{20}|^2 - 2M_{21}^2$, $C_{60} = M_{60} - 15M_{40}M_{20} + 30M_{20}^3$, $C_{63} = M_{63} - 9C_{42}C_{21} - 6C_{21}^3$. The theoretical values of the second, fourth, and sixth order cumulants of each modulation signal calculated are shown in Table 1.

Table 1. Theoretical value of cumulants of each order of MPSK and MQAM interference signals.

Modulation Type	C20	C21	C40	C41	C42	C60	C63
BPSK	E	E	2E ²	2E ²	2E ²	16E ³	13E ³
QPSK	0	E	E ²	0	E ²	0	4E ³
8PSK	0	E	0	0	E ²	0	4E ³
8QAM	0	E	1.15E ²	0	0.67E ²	3.44E ³	2.4E ³
16QAM	0	E	0.68E ²	0	0.68E ²	0	2.08E ³
64QAM	0	E	0.619E ²	0	0.619E ²	0	1.797E ³

It can be seen from Table 1 that the six modulation-type signals cannot be completely distinguished by high-order cumulants. Therefore, using the ratio of absolute values to construct the characteristic parameters to distinguish the six modulation types of signals in electromagnetic interference can not only eliminate the influence of signal amplitude change on the characteristic parameters, but also eliminate the influence of phase jitter

on the characteristic parameters. The four characteristic parameters are: $f_1 = |C_{41}|/|C_{42}|$, $f_2 = |C_{40}|/|C_{42}|$, $f_3 = |C_{63}|^2/|C_{42}|^3$, $f_4 = (|C_{42}|+|C_{40}|)/|C_{21}|^2$. The theoretical values of characteristic parameters of each modulation signal calculated are shown in Table 2.

Table 2. Characteristic parameter values of MPSK and MQAM interference signals characteristic parameters.

Characteristic Parameter	BPSK	QPSK	8PSK	8QAM	16QAM	64QAM
f_1	1	0	0	0	0	0
f_2	1	1	0	1.72	1	1
f_3	21.125	16	16	19.151	13.759	713.615
f_4	4	2	1	1.82	1.36	1.24

It can be seen from Table 2 that the f_1 characteristic parameter value of the BPSK signal is different from that of the other five modulation signals. Therefore, the modulation signal can be divided into BPSK and QPSK, 8PSK, 8QAM, 16QAM, and 64QAM by using f_1 characteristic parameters, so as to identify the BPSK signal; Using f_2 characteristic parameters, the modulation signal can be divided into three groups 8PSK, QPSK, 16QAM, 64QAM, and 8QAM, so as to identify 8PSK signal and 8QAM signal. Using the f_3 characteristic parameter, the modulation signal can be divided into QPSK, 16QAM, and 64QAM, so as to identify the QPSK signal. Finally, the 16QAM signal and the 64QAM signal can be identified by f_4 characteristic parameters. According to the above analysis, the characteristic parameters f_1 , f_2 , f_3 and f_4 of BPSK, QPSK, 8PSK, 8QAM, 16QAM, and 64QAM modulation signals are simulated and analyzed, respectively, so as to set the appropriate decision threshold to construct the decision tree classifier.

The parameters of the simulation environment are set as follows: carrier frequency is 1 MHz; sampling frequency is 6MHz; symbol rate is 1000 b/s; symbol length N is 3000; SNR = 0 dB~20 dB; noise is Gaussian white noise. Under the same SNR, 200 simulations are carried out, the average value is taken as the simulation value of the characteristic parameters of this modulated signal, and the simulation results are shown in Figure 2.

Figure 2a shows the simulation results of characteristic parameter f_1 . It can be seen that under different signal-to-noise ratios, the f_1 value of BPSK signals is maintained at about 1, while the f_1 value of the QPSK, 8PSK, 8QAM, 16QAM, and 64QAM signals is maintained in the range of 0 to 0.2. With the increase in signal-to-noise ratio, the f_1 value of five signals gradually tends to 0. Therefore, setting the decision threshold to 0.6 can identify BPSK signals.

Figure 2b shows the simulation results of characteristic parameter f_2 . It can be seen that the f_2 value of the 8PSK signal remains in the range of 0 to 0.2 and gradually tends to 0. The f_2 value of QPSK, 16QAM, and 64QAM signals is about 1, while the f_2 value of the 8QAM signal is about 1.7. Therefore, the 8PSK signal and the 8QAM signal can be recognized by setting the decision threshold to 1.4 and 0.5, respectively.

Figure 2c shows the simulation results of the characteristic parameter f_3 . It can be seen that the f_3 value of QPSK is about 16, the values of 16QAM and 64QAM are kept between 14 and 13.5, and the QPSK signal can be recognized by setting the decision threshold value to 15.

Figure 2d shows the simulation values of the characteristic parameter f_4 . It can be seen that the f_4 value of 16QAM and 64QAM is relatively close, and the value increases with the increase in signal-to-noise ratio. This is because the cumulant values of each order of 16QAM and 64QAM signals are relatively close, and the two signals are seriously affected by noise due to their large order. Therefore, it is difficult to distinguish the two signals by setting the decision threshold.

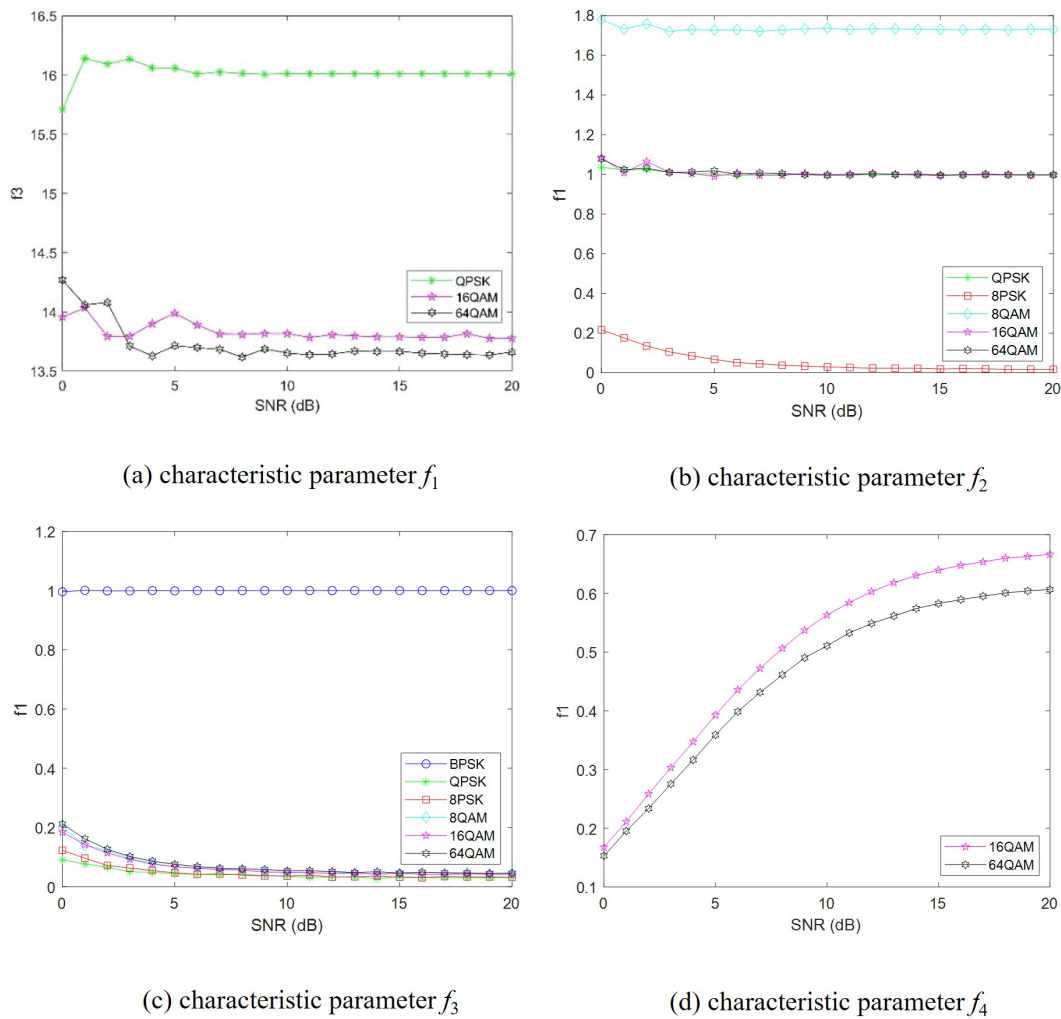


Figure 2. Simulation results of different characteristic parameter.

According to Equation (12), when the constellation phase offset is very small, i.e., $\theta = 0$, the MQAM signal can be expressed.

$$\begin{aligned}
 r(k) &= s(k) + n(k) \\
 &= [s_I(k) + n_I(k)] + j[s_Q(k) + n_Q(k)]
 \end{aligned}
 \tag{21}$$

The order of $r(k)$ is reduced once, and a new signal sequence $r'(k)$ is obtained.

$$\begin{aligned}
 r'(k) &= |\text{Re}[s(k) + n(k)]| + j|\text{Im}[s(k) + n(k)]| \\
 &= |s_I(k) + n_I(k)| + j|s_Q(k) + n_Q(k)| \\
 &= Y_I(k) + jY_Q(k)
 \end{aligned}
 \tag{22}$$

Under the condition of high signal-to-noise ratio, the probability density function of $Y_I(k)$ is approximately.

$$f_{Y_I[k]}(y) \approx \frac{1}{\sqrt{\pi N_0}} \exp \left[-\frac{(y - |s_I(k)|)^2}{N_0} \right]
 \tag{23}$$

where $Y_I(k)$ approximately obeys the Gaussian distribution with mean value $|s_I(k)|$ and variance $N_0/2$. Similarly, $Y_Q(k)$ also approximately obeys the Gaussian distribution with a mean value of $|s_Q(k)|$ and a variance of $N_0/2$. Therefore, the signal $r'(k)$ can be expressed .

$$\begin{aligned}
 r'(k) &= (|\operatorname{Re}[s(k)] + n_I(k)|) + j(|\operatorname{Im}[s(k)] + n_Q(k)|) \\
 &= (|s_I(k)| + j|s_Q(k)|) + n(k) \\
 &= s'(k) + n(k)
 \end{aligned} \tag{24}$$

The new signal can be calculated from Equation (24), and the order of the new signal becomes one quarter of the original signal, that is, $M' = M/4$, which realizes the order reduction processing of the signal. After the reduced order processing, the values of the characteristic parameters f_4 of the 16QAM signal and the 64QAM signal are shown in Figure 3.

As can be seen from Figure 3, with the increase in signal-to-noise ratio, the f_4 value gap between the two signals gradually becomes larger, and the f_4 value of 64QAM gradually stabilizes at about 2.26. Therefore, by setting the decision threshold to 2.27, respectively, the 16QAM signal and the 64QAM signal can be distinguished.

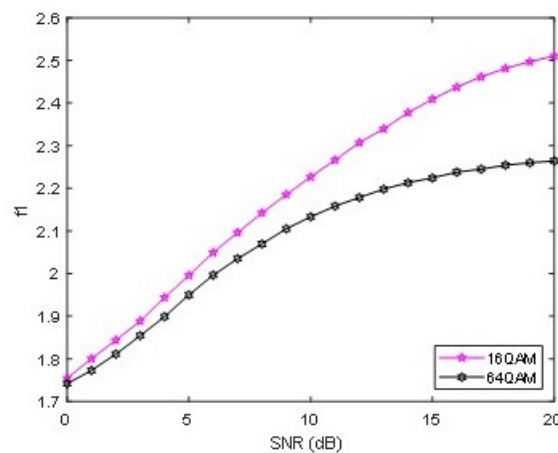


Figure 3. Simulation results of characteristic parameter f_4 after order reduction processing.

4. Signal Modulation Recognition System Based on SDR

HackRF One is used as the hardware platform for receiving electromagnetic interference modulation signals, and the frequency and symbol rate of the signals are estimated by the GNU Radio software to complete the clock synchronization and matching filtering; real-time performance needs to be taken into account in the actual engineering applications, so the modulation recognition algorithm based on the higher-order cumulative quantity is used to achieve modulation recognition and complete the phase correction of the signals, and finally the signal constellation diagram is combined with the system. The recognition result of the system is discriminated.

The HackRF One hardware structure is shown in Figure 4. The received signal passes through the antenna into the radio frequency circuit, through the programming settings, which determine whether the signal is amplified by a 14 dB amplifier, through the RFFC5072 chip to complete the signal mixing process, in which it will be changed into an intermediate frequency signal, and then through the MAX2837 chip, where it will be changed into an intermediate frequency signal mixing baseband IQ signals, then through the MAX5864 chip to the IQ signal by the sampling, where it will become a baseband digital signal (MAX5864 is responsible for the signal for ADC/DAC sampling process, sampling frequency of 22 MHz, sampling accuracy of 8bit); and then by the CPLD controller, which is responsible for the baseband signal. Then, the CPLD controller, responsible for the baseband signal timing control, behind the MAX5864, plays a role in buffering the data and controls the role of the transmission channel switch. Finally, the signal reaches the LPC4320/4330 processor, where the signal will be converted to data and through the USB interface into the PC and the GNU Radio software for communication.

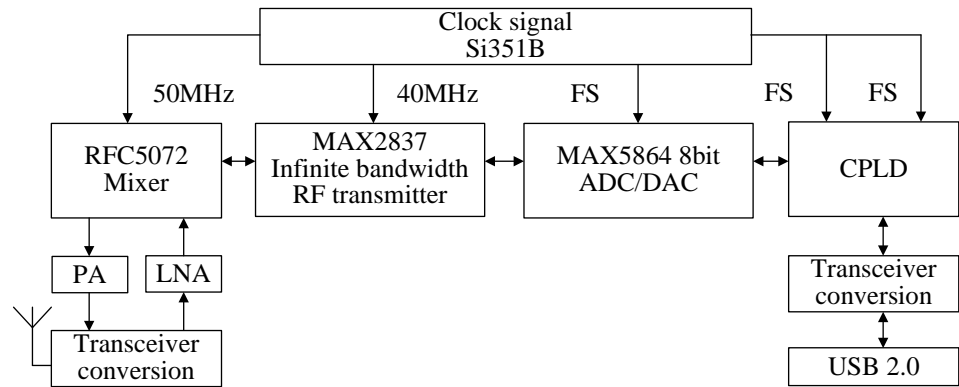


Figure 4. HackRF One hardware structure diagram.

The received signal enters the RF circuit through the antenna, and it is set whether to amplify the signal through programming. Then, the signal is down converted twice through the rfc5072 chip and max2837 chip to convert it into an analog baseband signal. Based on the GNU radio platform, the GRC flow diagram of electromagnetic interference signal modulation identification is designed and built, as shown in Figure 5. The functions of each module are as follows.

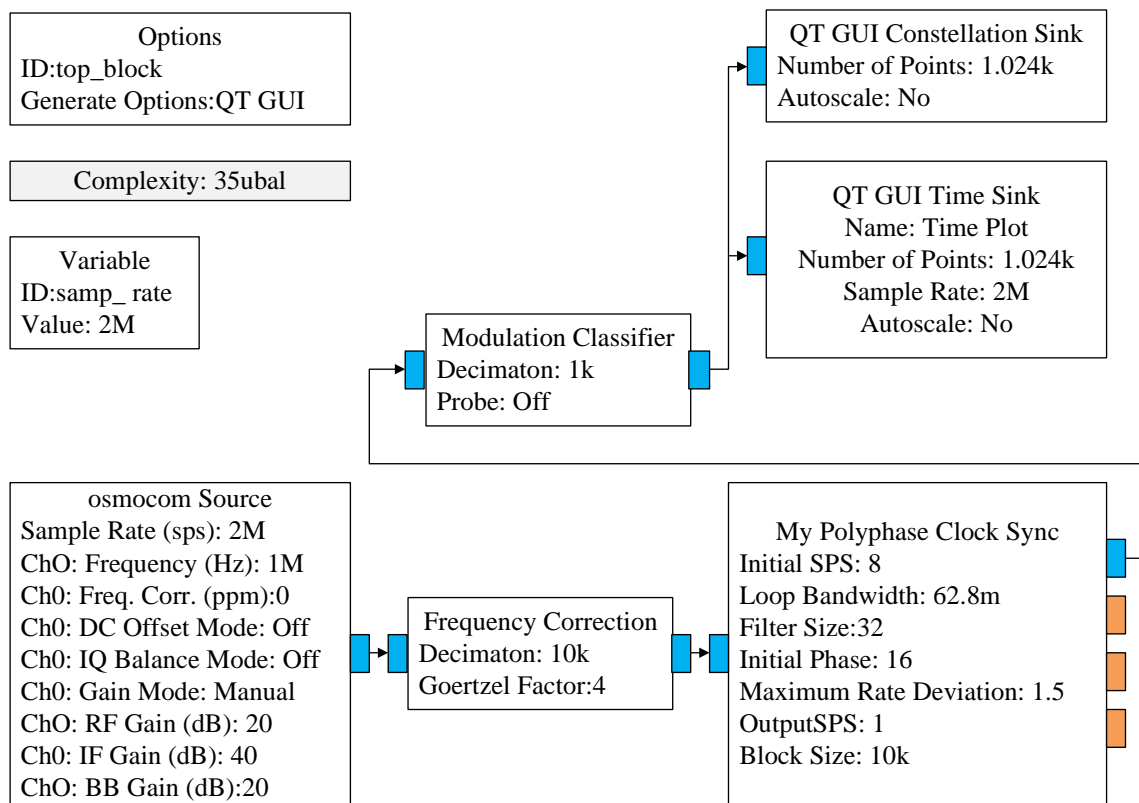


Figure 5. GRC flow chart of interference recognition syste.

Osmocom source: Receiving module. Connects the hardware of HackRF One with GNU radio software platform, and sends the electromagnetic interference modulation signal received by HackRF One to the software platform for processing.

Frequency correction: Frequency correction module. Estimates the frequency and symbol rate of the received signal and completes the frequency correction of the signal. At the same time, the number of samples for each symbol is obtained according to the estimated symbol rate, and it is passed to the next module as a stream label.

Polyphase clock sync: Clock synchronization module. Modifies the clock synchronization module provided by GNU Radio. The number of samples per symbol marked in the stream label of the previous module is used.

Modulation classifier: Classification and identification module. Carries out feature extraction on the signal, and completes classification and recognition.

QT GUI time sink: Visualization module. Displays the time domain waveform of the signal.

QT GUI constellation sink: Visualization module. Displays signal constellation.

5. Experimental Results and Analysis

In order to test the performance of the modulation recognition system based on software radio, the modulation recognition system test platform is built in the laboratory, as shown in Figure 6, the distance between the AV1445 signal generator and the receiver. The HackRF One hardware is about 6 m, and the HackRF One hardware is connected to the PC host computer through the USB2.0 interface, and on the PC side, the Ubuntu 18.04 system is equipped with the GNU Radio software platform, the electromagnetic interference signal is sent by the signal source, and the identification system receives the signal for processing and modulation identification.

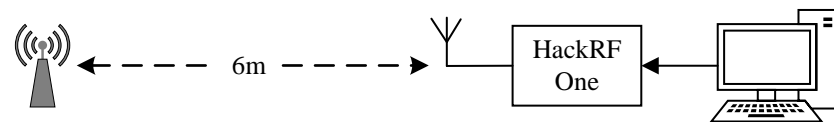


Figure 6. Structure diagram of system test platform.

The signal source generates six kinds of signals: BPSK, QPSK, 8PSK, 8QAM, 16QAM, and 64QAM, and runs the GRC flow chart to make the whole system is in a working state. The HackRF One hardware is used as the receiver to receive the signal, the received signal is down-converted and analog-to-digital converted into a baseband digital signal, and then the processed signal is sent to the PC. The signal pre-processing and classification are realized through the module in the GNU Radio software, and finally the recognition results are displayed.

When the signal generator sends out different modulation signals, the recognition results of the system are displayed through the time-domain waveform and constellation of the signal. The time-domain waveform and constellation of different modulation signals are obtained through the test, as shown in Figure 7. In Figure 7, the recognition result is passed, is marked in the time domain waveform by det-mod, and the identified interference signal type is compared with the constellation mapped by the interference signal.

When the recognition results are BPSK, QPSK, and 8PSK, 2, 4, and 8 signal points are equally spaced on the unit circle in the corresponding constellation. When the recognition result is 8QAM, 8 signal points in the corresponding constellation are distributed in a star shape. The constellation points of these four signals are obviously different, and the constellation map results are relatively clear. When the recognition results are 16QAM and 64QAM, 16 and 64 signal points in the corresponding constellation are square distributed, respectively.

Due to the large number of constellation points of the 16QAM signal and the 64QAM signal and the fact that the adjacent constellation points are close, the two signals will be more seriously affected by environmental noise, and the constellation points are easy to overlap. The experimental results show that the recognition results of the six modulation types of interference signals are consistent with the constellation, so the electromagnetic interference detection and recognition system meets the design requirements.

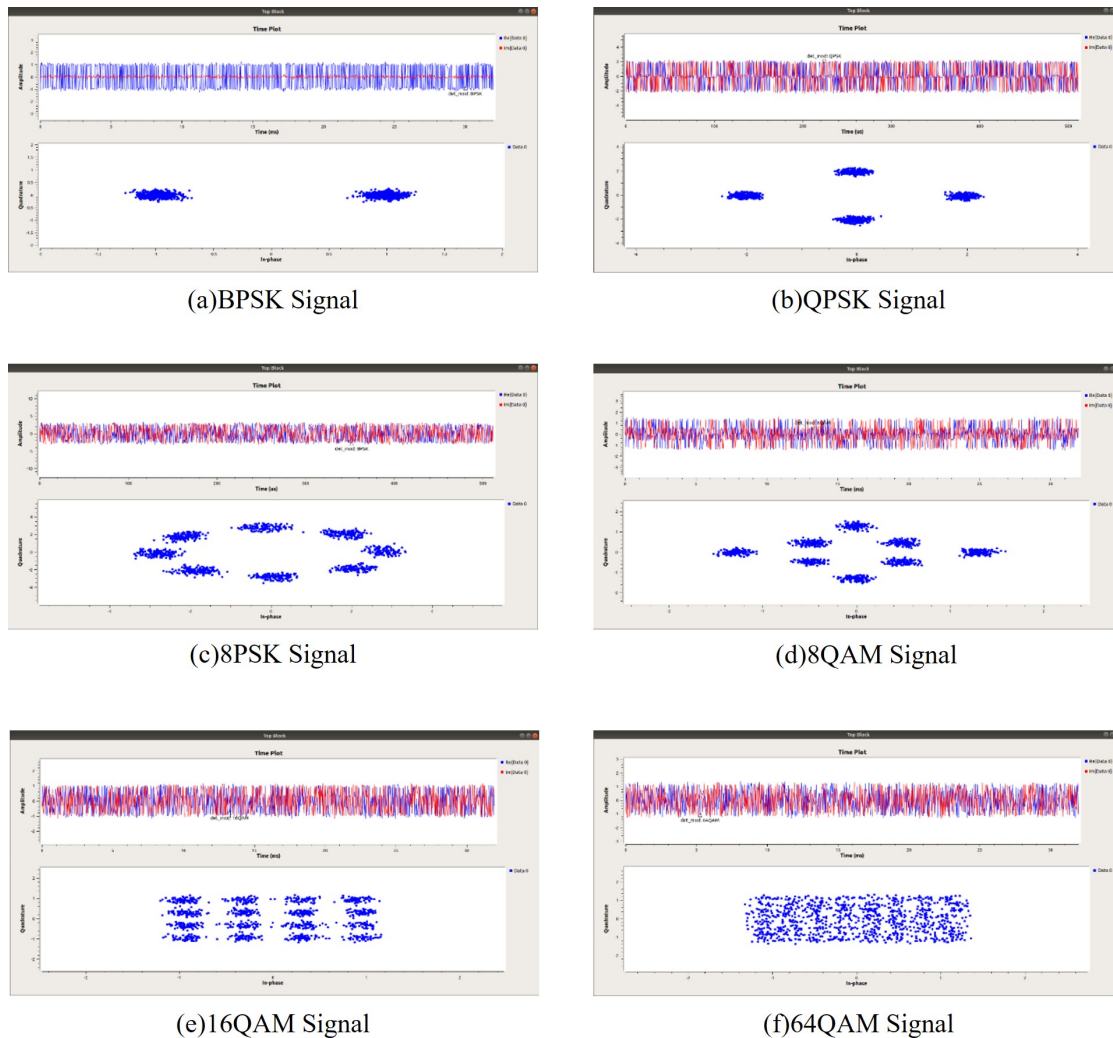


Figure 7. Time domain waveform and constellation of each interference signal.

In order to further verify the recognition performance of the system, the signal generator is used to generate six kinds of modulation signals, respectively, test each type of modulation signal for 100 times, and count the recognition results of each modulation signal to obtain the accuracy of the test results of each modulation signal, as shown in Table 3.

Table 3. Phase estimation parameters of each interference signal.

Modulation Type	Accuracy (%)
BPSK	100
QPSK	99
8PSK	94
8QAM	98
16QAM	93
64QAM	90

It can be seen from Table 3 that in the test of the actual environment, the recognition results of the system for six modulation signals can reach more than 90%, with high accuracy, which is basically consistent with the simulation results. Therefore, the modulation recognition system based on software radio meets the design requirements.

6. Conclusions

Considering the problem of modulation type interference signal recognition, a modulation mode recognition system of electromagnetic interference signal based on software radio was designed. The system receives the interference signal through HackRF One hardware, and realizes the frequency and symbol rate estimation, clock synchronization, classification recognition, and phase correction of the received signal in the GNU Radio software platform. Finally, the recognition results are intuitively reflected through a domain waveform diagram and constellation diagram. The results show that the system can quickly and accurately identify the modulation type of the electromagnetic interference signal. Compared with the traditional communication signal modulation identification method, the identification result is more real-time and more suitable for practical engineering applications.

Author Contributions: All authors have the same contributions. All authors have read and agreed to the published version of the manuscript.

Funding: This research was funded by Research on Key Methods of Internet of Things Security Situational Awareness in Open Pit Mines (LJKMZ20220677).

Data Availability Statement: This paper did not use publicly available datasets.

Conflicts of Interest: The authors declare no conflict of interest.

References

1. Same, M.H.; Gandubert, G.; Ivanov, P.; Landry, R., Jr.; Gleeton, G. Effects of interference and mitigation using notch filter for the DVB-S2 standard. *Telecom* **2020**, *1*, 242–265. [[CrossRef](#)]
2. Moysis, L.; Volos, C.; Stouboulos, I.; Goudos, S.; Çiçek, S.; Pham, V.-T.; Mishra, V.K. A novel chaotic system with a line equilibrium: Analysis and its applications to secure communication and random bit generation. *Telecom* **2020**, *1*, 283–296. [[CrossRef](#)]
3. Kim, K.; Polydoros, A. Digital modulation classification: The BPSK versus QPSK case. In Proceedings of the MILCOM 88, 21st Century Military Communications-What's Possible?. Conference record. Military Communications Conference, San Diego, CA, USA, 23–26 October 1988; Volume 2, pp. 431–436.
4. Lay, N.E.; Polydoros, A. Modulation classification of signals in unknown ISI environments. In Proceedings of the IEEE Military Communications Conference, San Diego, CA, USA, 5–8 November 1995; pp. 170–174.
5. Panagiotou, P.; Anastasopoulos, A.; Polydoros, A. Likelihood ratio tests for modulation classification. In Proceedings of the MILCOM 2000 Proceedings. 21st Century Military Communications. Architectures and Technologies for Information Superiority, Los Angeles, CA, USA, 22–25 October 2000; Volume 2, pp. 670–674.
6. Dobre, O.A.; Hameed, F. Likelihood-Based Algorithms for Linear Digital Modulation Classification in Fading Channels. In Proceedings of the 2006 Canadian Conference on Electrical and Computer Engineering, Ottawa, ON, Canada, 7–10 May 2006; pp. 1347–1350.
7. Wu, B.; Yuan, Y.B.; Wang, B. Maximum Likelihood Modulation Recognition for Continuous Phase Modulation Signals Using Memory Factor. *J. Electron. Inf. Technol.* **2016**, *38*, 2546–2552.
8. Wang, L.X.; Guo, S.T.; Jia, C.J. Recognition of digital modulation signals based on wavelet amplitude difference. In Proceedings of the 2016 7th IEEE International Conference on Software Engineering and Service Science (ICSESS), Beijing, China, 26–28 August 2016; pp. 627–630.
9. Chen, J.L.; Xiong, G. A Modulation Recognition Method based on New Feature and SVM. *Commun. Technol.* **2018**, *51*, 763–767
10. Liu, Y.; Shan, H.; Hu, Y.H.; Wang, Y. Automatic Recognition Based on Spectral Feature in Satellite Communication. *Fire Control. Command. Control.* **2017**, *42*, 45–48+53.
11. Chen, Z.Y. A Combined Modulation Recognition Based on Cyclic Spectrum and High-order Cumulants. *Telecommun. Eng.* **2015**, *55*, 328–332.
12. Wang, H.; Guo, L.L. A New Method of Automatic Modulation Recognition Based on Dimension Reduction. In Proceedings of the 2017 Forum on Cooperative Positioning and Service (CPGPS), Harbin, China, 19–21 May 2017; pp. 316–320.
13. Wang, L.; Ren, Y. Recognition of digital modulation signals based on high order cumulants and support vector machines. In Proceedings of the 2009 ISECS International Colloquium on Computing, Communication, Control, and Management, Sanya, China, 8–9 August 2009; pp. 271–274.
14. Swami, A.; Sadler, B.M. Hierarchical digital modulation classification using cumulants. *IEEE Trans. Commun.* **2000**, *48*, 416–429. [[CrossRef](#)]
15. Zhang, L.; Li, Q. Research on modulation recognition algorithm based on higher-order cumulant. *J. Inf. Eng. Univ.* **2017**, *18*, 403–408.

16. Weng, J.X.; Zhao, Z.J.; Zhan, J.M. Modulation type recognition algorithm based on combination of multiple higher order cumulant. *J. Hangzhou Dianzi Univ. (Natural Sci.)* **2019**, *39*, 1–5.
17. Ali, A.K.; Erelebi, E. An M-QAM Signal Modulation Recognition Algorithm in AWGN Channel. *Sci. Program.* **2019**, *2019*, 1–17. [[CrossRef](#)]
18. Yuan, L.; Ning, S.; He, Y.; Lu, J.; Lv, M. Modulation recognition method based on high-order cumulant feature learning. *Syst. Eng. Electron.* **2019**, *41*, 2122–2133.
19. Liu, Z.Y.; Wang, A.Y.; Li, R. A method of non-cooperative communication signals feature extraction. *J. Xian Univ. Sci. Technol.* **2020**, *40*, 706–711.
20. Liu, Q.P.; Gao, X.Y.; Qiu, X. Automatic modulation recognition based on USRP. *Comput. Appl. Softw.* **2020**, *37*, 110–114.

Disclaimer/Publisher’s Note: The statements, opinions and data contained in all publications are solely those of the individual author(s) and contributor(s) and not of MDPI and/or the editor(s). MDPI and/or the editor(s) disclaim responsibility for any injury to people or property resulting from any ideas, methods, instructions or products referred to in the content.